

## Original Research

# Histologic Comparison of the Dura Mater among Species

Ahmet Kinaci,<sup>1,2,\*</sup> Wilhelmina Bergmann,<sup>3</sup> Ronald LAW Bleys,<sup>4</sup> Albert van der Zwan,<sup>1,2</sup> and Tristan PC van Doormaal<sup>1,2,5</sup>

The biocompatibility, biodegradation, feasibility, and efficacy of medical devices like dural sealants and substitutes are often evaluated in various animal models. However, none of these studies explain the rationale for choosing a particular species, and a systematic interspecies comparison of the dura is not available. We hypothesized that histologic characteristics of the dura would differ among species. We systematically investigated basic characteristics of the dura, including thickness, composition, and fibroblast orientation of the dura mater, in 34 samples representing 10 animal species and compared these features with human dura by using hematoxylin and eosin staining and light microscopy. Dura showed many similarities between species in terms of composition. In all species, dura consisted of at least one fibrovascular layer, which contained collagen, fibroblasts, and blood vessels, and a dural border cell layer beneath the fibrovascular layer. Differences between species included the number of fibrovascular layers, fibroblast orientation, and dural thickness. Human dura was the thickest (564  $\mu\text{m}$ ) followed by equine (313  $\mu\text{m}$ ), bovine (311  $\mu\text{m}$ ), and porcine (304  $\mu\text{m}$ ) dura. Given the results of this study and factors such as gross anatomy, feasibility, housing, and ethical considerations, we recommend the use of a porcine model for dural research, especially for in vivo studies.

**Abbreviation:** DBC, dural border cell

**DOI:** 10.30802/AALAS-CM-19-000022

The dura mater is the outermost layer of the meninges that cover the CNS. Dura has important roles as a protective barrier against mechanical force and infection as well as other complex functions.<sup>2,8,23,34</sup> Human cranial dura mater consists of 3 layers: the periosteal layer, meningeal layer, and dural border cell (DBC) layer. The periosteal layer, the outermost layer, is attached to the inner skull and contains vessels and nerves. It consists of elongated fibroblasts with large intercellular spaces. The meningeal layer is the middle layer and contains more fibroblasts and proportionally less collagen than the periosteal layer. The innermost layer of the dura is the DBC layer, which also is called the mesothelial layer, neurothelium, superficial zone, inner dural cell layer, subdural cell layer, or dural limiting layer.<sup>1</sup> Compared with the meningeal layer, the DBC layer has flattened fibroblasts with relatively few intercellular junctions and a lack of extracellular collagen and extracellular spaces of various sizes and shapes.<sup>14,22,24,32</sup> The periosteal and meningeal layers are tightly adhered to each other, except at the height of the dural venous sinuses and the cranial reflections (falx cerebri, falx cerebelli, and tentorium), which are formed by the meningeal layer only.<sup>1,4,13,29</sup>

In neurosurgical practice, dural substitutes and sealants are commonly used to ensure watertight closure of the dura. The efficacy, biocompatibility, and degradation of such medical devices are evaluated in various in vitro and in vivo studies, which also are necessary for regulatory approval. Bovine, canine, caprine, equine, feline, leporine, murine, porcine, and ovine dura models have been used.<sup>3,6,7,9,17-19,21,31</sup> However, none of these studies compared various species or explained the rationale underlying the choice of a particular species, even though dural characteristics may influence the results regarding dural closure and the leakage of CSF. We hypothesized that various histologic features of dura—including thickness, composition, orientation of cells, and vascularization—would differ between species. The 2 main objectives of this study were to 1) histologically analyze the cranial dura of various species used in ex vivo and in vivo studies and 2) compare the dural features of animal species with human cranial dura.

## Materials and Methods

Pigs, rats, horses, rabbits, cows, sheep, goats, cats, and dogs were used at a dural model in at least 1 study each.<sup>3,5-7,9,11,17-21,30,31</sup> Dural samples from 4 pigs, 4 cows, 3 goats, 3 rabbits, 3 sheep, 3 horses, 4 dogs, 3 cats, and 4 rats were harvested at necropsy from animals referred to the Division of Pathology (Faculty of Veterinary Medicine, Utrecht University) as surplus laboratory animals of the Faculty of Veterinary Medicine (Utrecht University) or from animals at the slaughterhouse. No approval was needed from the animal welfare committee or medical research ethics committee for this study.

All 3 samples of human dura were obtained through the donation program at the Department of Anatomy of the University

Received: 15 Feb 2019. Revision requested: 01 Apr 2019. Accepted: 30 Apr 2019.

<sup>1</sup>Department of Neurology and Neurosurgery, Brain Center Rudolph Magnus, University Medical Center Utrecht, Utrecht, The Netherlands; <sup>2</sup>Brain Technology Institute, Utrecht, The Netherlands; <sup>3</sup>Division of Pathology, Faculty of Veterinary Medicine, Utrecht University, Utrecht, The Netherlands; <sup>4</sup>Department of Anatomy, University Medical Center, Utrecht University, Utrecht, The Netherlands; <sup>5</sup>Department of Neurosurgery, University Hospital Zurich, University of Zurich, Zurich, Switzerland; Clinical Neuroscience Center, University Hospital Zurich, University of Zurich, Zurich, Switzerland.

\*Corresponding author. Email: akinaci@outlook.com

Medical Center Utrecht. Written informed consent was obtained from donors during life that allowed the use of their entire bodies for educational and research purposes. We harvested the dura at a standardized location (Figure 1) The samples of dura were harvested within 24 h after death, fixed in 4% neutral buffered formaldehyde solution, routinely processed for histologic examination, and stained with hematoxylin and eosin. Dura of the rat and rabbit were harvested and fixed together with the skull as the dura was very thin and tightly attached to the skull. A veterinary pathologist (WB) using light microscopy assessed samples in terms of mean thickness, number of visible layers, composition, vascularization, and fibroblast orientation. The mean dural thickness was calculated based on 10 measurements per species because the dura varied in thickness, even in the same sample. When the fibrovascular layer comprised 2 layers, the layers were distinguished as periosteal and meningeal layers. However, when 2 layers were indistinguishable, we simply called it the fibrovascular layer. A single representative histologic image was acquired per species, and we could not show all dural characteristics in a single image.

Significance between categorical and continuous data was tested by using the Mann–Whitney U or Kruskal–Wallis test.

## Results

We analyzed 34 samples, representing 10 different species. The main characteristics of dura (mean thickness, number of visible layers and cellular orientation of the different layers) are shown in Table 1 A representative histologic image was obtained for each species (Figures 2 through 11).

It was not possible to show all characteristics in a single image.

Human dura consisted of 3 distinctive dural layers (periosteal, meningeal, and DBC layers) with a mean thickness ( $\pm 1$  SD) of  $564 \pm 50 \mu\text{m}$ . Cells were slightly haphazardly oriented in both the periosteal and meningeal layers. The meningeal layer contained substantially more fibroblasts per unit area, compared with the periosteal layer. The DBC layer was visible and had a mean thickness of 3 to 8 cells. This layer was irregularly thick and sinuous. Large blood vessels were distributed mainly in the periosteal layer, whereas small blood vessels (maximum diameter,  $42 \mu\text{m}$ ) were located within the border between the meningeal and DBC layers (Figure 2).

Bovine dura had a mean thickness of  $311 \pm 87 \mu\text{m}$ . Multifocally, all 3 layers could be distinguished. The orientation of the fibroblasts in the periosteal layer was longitudinal, whereas the orientation of the cells of the meningeal layer was more oblique. The number of fibroblasts per unit area was higher in the meningeal layer than in the periosteal layer. The DBC layer had a mean thickness of 3 to 8 cells, which were irregular and without invagination. Blood vessels were present mainly between the periosteal and meningeal layers and at the upper border of the periosteal layer. The maximum diameter of the vessels was  $112 \mu\text{m}$ . Compared with human dura, bovine dura was markedly thinner, fibroblasts had a more organized orientation, and the bovine meningeal layer seemed to be more cellular than its human counterpart. In addition, the bovine DBC layer showed more irregularity compared with human dura (Figure 3).

Canine dura had a mean thickness of  $233 \pm 71 \mu\text{m}$ . All 3 layers were visible, with slightly haphazard orientation of the fibroblasts in the periosteal layer and longitudinal orientation in the meningeal layer. The fibroblasts in the meningeal layer were slightly more haphazard than in the periosteal layer. The DBC layer had a mean thickness of 3 to 6 cells and was regular. The blood vessels were situated at the periphery of the meningeal layer, with a maximum thickness of  $27 \mu\text{m}$ . Compared with

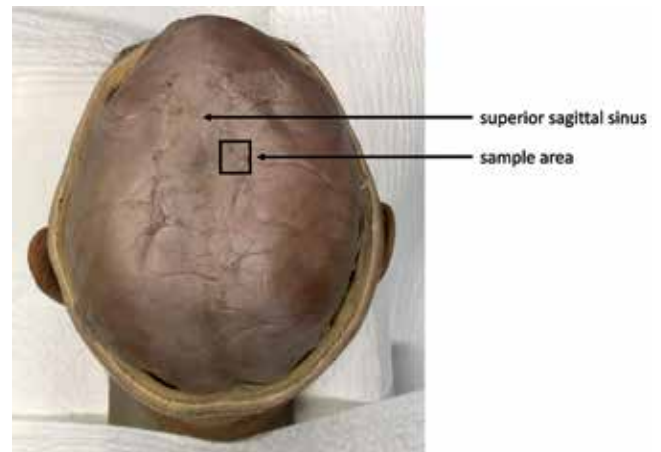


**Figure 1.** As shown in the figure, the dura was harvested parasagittally in all species.

human dura, canine dura was significantly thinner and more longitudinally oriented, and its blood vessels were situated in the meningeal layer, toward the DBC layer (Figure 4).

Caprine dura had a mean thickness of  $284 \pm 57 \mu\text{m}$ . Within the tissues examined, a single fibrovascular and DBC layer was visible. The orientation of the fibroblasts in the fibrovascular layer was longitudinal. The DBC layer had a mean thickness of 2 to 5 cells. The blood vessels mostly were situated at the periosteal border toward the cranium. The maximal diameter of the vessels was  $74 \mu\text{m}$ . Compared with human, the caprine dura was significantly thinner, its fibroblasts were longitudinally oriented, it had proportionally more fibroblasts per unit area, and the blood vessels were more often in the upper periosteal border. The DBC layer was more regular than in humans (Figure 5).

Equine dura had a mean thickness of  $313 \pm 64 \mu\text{m}$ . A single fibrovascular and the DBC layer were visible. The orientation of the fibroblasts in fibrovascular layer was longitudinal and became slightly haphazardly toward the DBC layer. The proportion of fibroblasts increased toward the inner border, without a demarcated border. The DBC layer was irregular, 4 to 8 cells wide, sinuous, and invaginated. Blood vessels (maximum diameter,  $44 \mu\text{m}$ ) were visible at the periphery of both borders and occasionally in the middle of the dura. Compared with human dura, only 2 layers were visible on light microscopy, and equine dura was significantly thinner. In addition, the blood vessels were more peripherally situated and the DBC was more irregular and sinuous, compared with human dura (Figure 6).

Feline dura had a mean thickness of  $201 \pm 78 \mu\text{m}$ . All 3 layers were visible. The orientation of fibroblasts was slightly haphazard in the periosteal layer and longitudinal in the meningeal layer. The DBC was mainly regular, 3 to 6 cells wide. Blood vessels were present mainly between the meningeal and DBC layers; fewer vessels were present between the periosteal and meningeal layers. The maximum diameter of the blood vessels was  $88 \mu\text{m}$ . Compared with human dura, feline dura was significantly thinner, the orientation of fibroblasts more organized, and more blood vessels were present between the meningeal and DBC layers. The feline DBC layer was more regular and thinner compared with human dura (Figure 7).

Leporine dura had a mean thickness of  $99 \pm 32 \mu\text{m}$ . All 3 layers were distinguishable through light microscopy. The fibroblasts in the periosteal layer were slightly haphazardly orientated. In the meningeal layer, the fibroblasts were orientated longitudinally. The DBC layer was regular and sinuous, without invagination, and 3 to 5 cells wide. Most blood

**Table 1.** Histologic characteristics of the dura according to species

	No. of samples	Dural thickness (µm)		No. of layers	Fibroblast orientation		
		mean	1 SD		no distinguishable layers	periosteal layer	meningeal layer
Human	3	564	50	3	—	slightly haphazard	slightly haphazard
Cow	4	311	87	3	—	longitudinal	longitudinal
Cat	3	201	78	3	—	slightly haphazard	longitudinal
Dog	4	233	71	3	—	slightly haphazard	longitudinal
Goat	3	284	57	2	longitudinal	—	—
Horse	3	313	64	2	slightly haphazard	—	—
Pig	4	304	77	3	—	slightly haphazard	longitudinal
Rabbit	3	99	32	3	—	slightly haphazard	longitudinal
Rat	4	49	15	2	slightly haphazard	—	—
Sheep	3	234	91	2	slightly haphazard	—	—



**Figure 2.** Human dura mater.

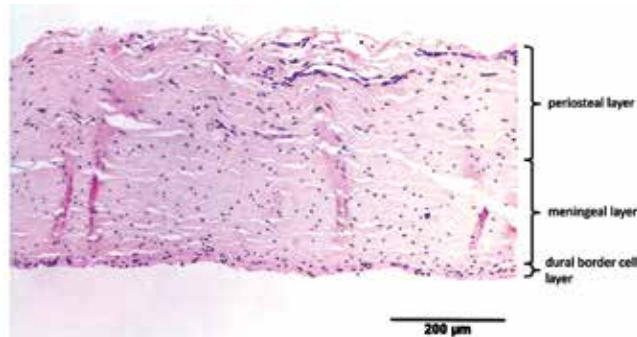


**Figure 3.** Bovine dura mater.

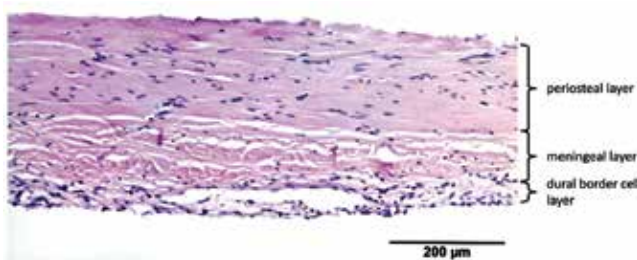


**Figure 4.** Canine dura mater.

vessels (maximal diameter, 65 µm) were oriented at the periosteal upper border and between the meningeal and DBC layers. Compared with human dura, leporine dura was significantly thinner, the orientation of the fibroblasts of the meningeal layer was more organized, and more blood vessels were present at the periosteal upper border. The DBC layer of leporine dura was thinner and more regular compared with human dura (Figure 8).

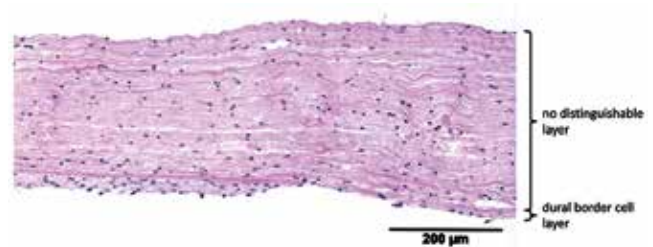


**Figure 5.** Caprine dura mater. The DBC layer is partially visible.

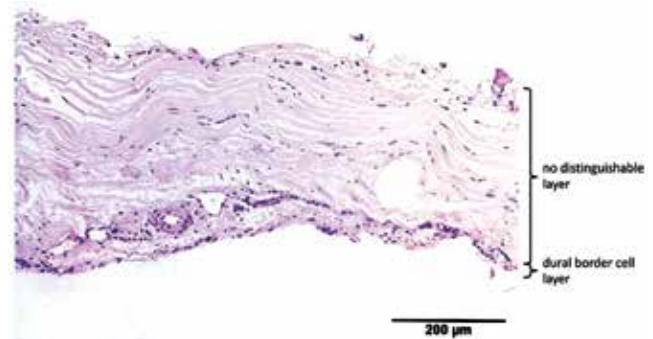


**Figure 6.** Equine dura mater.

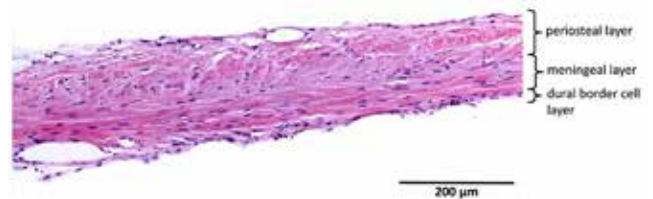


**Figure 7.** Feline dura mater.

Murine dura had a mean thickness of 49 ± 15 µm. A single fibrovascular layer and a DBC layer were visible. The fibroblasts in the fibrovascular layer were slightly haphazardly oriented. The DBC layer was 2 to 4 cells wide and regular, without invagination. The blood vessels (maximum diameter, 20 µm) were situated in the upper border. Compared with human dura, murine dura was significantly thinner and contained fewer fibroblasts and blood vessels. The DBC layer was thinner and more regular than human dura (Figure 9).

Ovine dura had a mean thickness of 234 ± 91 µm. In the tissues examined, only one fibrovascular layer and a DBC layer were visible. The orientation of the fibroblasts was slightly

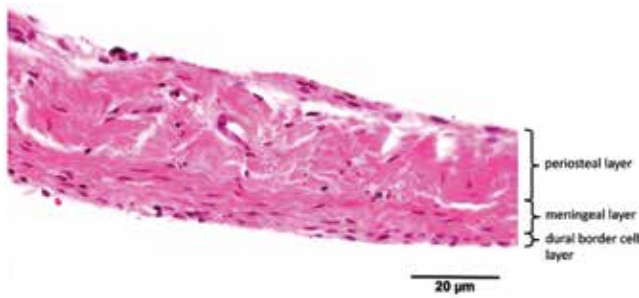


Figure 8. Leporine dura mater.

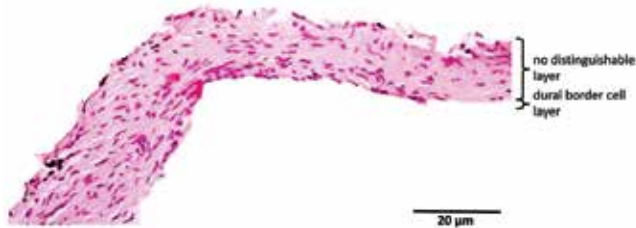


Figure 9. Murine dura mater. The DBC layer is partially visible.

haphazard. The DBC layer was 2 to 3 cell layers wide, regular, and without invagination. The blood vessels (maximum diameter, 32  $\mu\text{m}$ ) were commonly present at the border with the DBC layer. Compared with human dura, ovine dura consisted of only 2 layers and was significantly thinner. In addition, the ovine DBC layer was more regular and without invagination compared with human (Figure 10).

Porcine dura had a mean thickness of  $304 \pm 77 \mu\text{m}$ . All 3 dural layers were visible. The orientation of the fibroblasts was slightly haphazard for the periosteal layer and longitudinal for the meningeal layer. The DBC layer was irregular, 4 to 8 cells wide, and sinuous. The blood vessels (maximum diameter, 35  $\mu\text{m}$ ) were present mostly in the periphery of the periosteal layer and in the border between the meningeal and DBC layers. Compared with human dura, porcine dura was significantly thinner, and the orientation of the fibroblasts in the periosteal layer was slightly more organized (Figure 11).

The dura, composed mainly of collagen and fibroblasts, showed many similarities across species. In all species, blood vessels were present in the fibrovascular layer. The DBC layer could be identified in all species and was characterized by a high density of cells, with proportionally less extracellular matrix. Interspecies differences included the number of layers, dural thickness, and orientation of the fibroblasts. As in human dura, the fibrovascular layer of cows, cats, dogs, pigs, and rabbits had distinguishable periosteal and meningeal layers. The dura of goats, horses, rats, and sheep consisted histologically of a single fibrovascular layer. Equine dura showed a single fibrovascular layer but with an increase in fibroblasts toward the inner border without clearly separated layers, suggesting an intermediate form. In addition, the orientation of the fibroblasts within the different layers varied among the species examined (Table 1). In none of the animals with 2 fibrovascular layers was the fibroblast orientation exactly the same as in humans. Morphologic differences in the DBC layer were seen between species. In human dura, the DBC layer tended to be irregular and sinuous, whereas DBC layer of animals was more regular and less sinuous. Measurements showed that human dura (564  $\mu\text{m}$ ) was significantly ( $P < 0.05$ ) thicker than the dura in all other species. Human dura was almost 2 times thicker than the thickest dura among

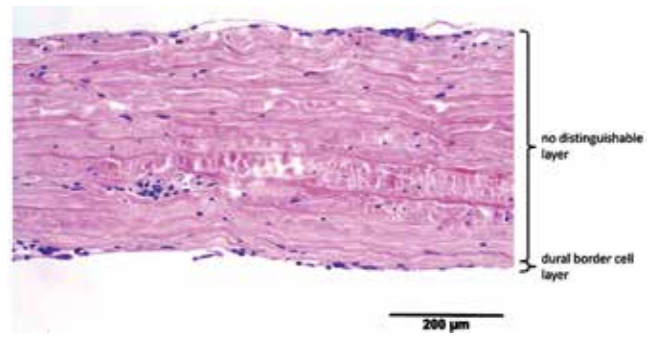


Figure 10. Ovine dura mater. The DBC layer is partially visible.

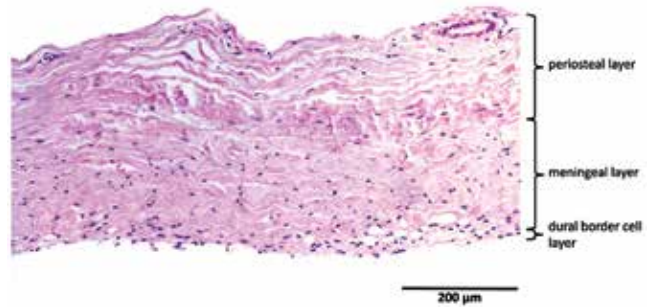


Figure 11. Porcine dura mater. The DBC layer is partially visible.

animals. Neither dural thickness nor number of dural layers differed among any species.

## Discussion

Here we describe the basic characteristics of the dura mater from 10 animal species that have been used in at least one study to evaluate dural sealants or substitutes. None of the prior studies described the dural characteristics of the selected species or compared them with human dura, although these features might influence the outcomes of these studies. Therefore, we analyzed the histologic morphology of the dura in these species and compared the dura in animals with human dura.

Histologically the dura showed many similarities and differences across the species evaluated. In all species, the dura consisted of 2 parts: the fibrovascular layer, which contained collagen, fibroblasts, and blood vessels, and the DBC layer, which was beneath the fibrovascular layer. Differences in dura between species involved the number of fibrovascular layers, dural thickness, and the orientation of the fibroblasts. The fibrovascular layer consisted of 1 or 2 layers. In humans, cows, cats, dogs, pigs, and rabbits, 2 layers (periosteal and meningeal layers) separated by a clear border were distinguishable in the fibrovascular layer. The 2 layers in these species were clearly distinguishable due to differences in the orientation and density of the fibroblasts in both layers. Equine dura consisted of a single fibrovascular layer but showed an increase of fibroblasts toward the inner border but without the clear border seen in species with 2 fibrovascular layers. In contrast, 3 species (goats, rats, and sheep) had a single, homogenous fibrovascular layer. However, it's unknown whether these species in fact have only one anatomic layer or whether 2 anatomic layers are visible as a single layer through light microscopy due to the same orientation and density of the fibroblasts in both layers. The presence of venous sinuses in these 3 species suggests that the second explanation might be the case, given that the venous sinuses form embryologically between these 2 layers.<sup>10,27,33</sup> Further studies should investigate this possibility.

Morphologic differences in the DBC layer were particularly marked between humans and the animal species. In humans, the DBC layer was more irregular and sinuous, whereas in animals, the DBC layer appeared more regular and less sinuous. This same observation was made in a previous study, which showed that the cells in the DBC layer of humans frequently appear sinuous or undulated and may interdigitate, whereas in animals, the cells usually form a more orderly layer with fewer irregularities.<sup>14</sup> Perhaps the DBC layer in humans becomes increasingly irregular as the dura thickens due to aging.

The measured dural thickness differed among species. This might be relevant in dural sealant and substitute studies, especially when the dura is closed with stitches. Although no studies have compared the CSF leakage rate among species, a thicker dura is less fragile and—theoretically—the risk of leakage through needle holes presumably is decreased. The dura of rats and rabbits were very fragile and could not be harvested for this study without prior fixation in formaldehyde. Therefore, despite their use in prior studies, we suggest that species like rats and rabbits should be avoided as dura models for in vitro or in vivo studies.<sup>15,26,28</sup>

Fibroblasts in the meningeal layer were longitudinally oriented in all species except humans, in which they were oriented slightly haphazardly. The orientation of the fibers in the dura mater and risk of CSF leakage seem to be related, although the exact mechanism is still unknown.<sup>12</sup> The longitudinal orientation of the fibroblasts suggests that the dura may be dissected more easily in one direction (that is, parallel to the fibers). This phenomenon can be seen in human spinal dura; the collagen fibers in human spinal dura are mostly longitudinally oriented.<sup>25</sup> This orientation might be the reason that the dura can be easily bluntly dissected from cranial to caudal, whereas dissection is not possible in the transverse direction.

The results of this study indicate that dura thickness differs significantly between species. This variable seems to be one of the most important determinants regarding the choice of the animal model. In terms of dura thickness, bovine, equine and porcine dura resembles closest to human dura. However, the choice of animal for in vitro or in vivo studies also depends on other factors, such as gross anatomy, availability, feasibility, handling, housing, and ethical considerations. In this context, bovine and equine models are less relevant, whereas the porcine model meets these factors favorably, especially for in vivo research.

This study had several limitations. First, despite that the attempt to harvest the dura from the same location in all species, precise determination of location was not always possible, particularly in small animals like rabbits and rats. The paramedian region in such small animals is only several millimeters in size, thus making precise localization difficult. In addition, fiber orientation could differ among regions.<sup>16</sup> Second, correctly embedding the material into the paraffin is a difficult task, with a risk of partial oblique cuts, leading to small variations in thickness. We attempted to address this issue by measuring the thickness at 10 different regions. Finally, the number of samples per species was relatively small; individual variances depending on race, sex, and age might occur.

In conclusion, the dura mater among the species examined showed many similarities regarding composition of the dura from a fibrovascular layer and a DBC layer. Differences in the dura were observed in regard to thickness, the number of fibrovascular layers, and the orientation of the fibroblasts. Given the results of this study and considering factors as gross anatomy, feasibility, housing, and ethical considerations, we recommend the use of a porcine model for dura research, especially for in vivo studies.

## Acknowledgments

This study was funded in part by Polyganics BV.

## References

1. **Adeeb N, Mortazavi MM, Tubbs RS, Cohen-Gadol AA.** 2012. The cranial dura mater: a review of its history, embryology, and anatomy. *Childs Nerv Syst* **28**:827–837. <https://doi.org/10.1007/s00381-012-1744-6>.
2. **Aspelund A, Antila S, Proulx ST, Karlsten TV, Karaman S, Detmar M, Wiig H, Alitalo K.** 2015. A dural lymphatic vascular system that drains brain interstitial fluid and macromolecules. *J Exp Med* **212**:991–999. <https://doi.org/10.1084/jem.20142290>
3. **Barbolt TA, Odin M, Leger M, Kangas L, Hoiste J, Liu SH.** 2001. Biocompatibility evaluation of dura mater substitutes in an animal model. *Neurol Res* **23**:813–820. <https://doi.org/10.1179/016164101101199405>.
4. **Bayot ML, Zabel MK.** 2019. *Neuroanatomy, brain, sinuses, dural venous sinuses*. Treasure Island (FL): StatPearls publishing.
5. **Bernards CM, Hill HF.** 1990. Morphine and alfentanil permeability through the spinal dura, arachnoid, and pia mater of dogs and monkeys. *Anesthesiology* **73**:1214–1219. <https://doi.org/10.1097/0000542-199012000-00020>.
6. **Chauvet D, Tran V, Mutlu G, George B, Allain JM.** 2011. Study of dural suture watertightness: an in vitro comparison of different sealants. *Acta Neurochir (Wien)* **153**:2465–2472. <https://doi.org/10.1007/s00701-011-1197-9>.
7. **Collins RL, Christiansen D, Zazanis GA, Silver FH.** 1991. Use of collagen film as a dural substitute: preliminary animal studies. *J Biomed Mater Res* **25**:267–276. <https://doi.org/10.1002/jbm.820250212>.
8. **Dando SJ, Mackay-Sim A, Norton R, Currie BJ, John JAS, Ekberg JAK, Batzloff M, Ulett GC, Beacham IR.** 2014. Pathogens penetrating the central nervous system: infection pathways and the cellular and molecular mechanisms of invasion. *Clin Microbiol Rev* **27**:691–726.
9. **Deng K, Ye X, Yang Y, Liu M, Ayyad A, Zhao Y, Yuan Y, Zhao J, Xu T.** 2016. Evaluation of efficacy and biocompatibility of a new absorbable synthetic substitute as a dural onlay graft in a large animal model. *Neurol Res* **38**:799–808. <https://doi.org/10.1080/01616412.2016.1214418>.
10. **Dou L, Yu W.** 2017. Expression of NF-E2-related factor 2 in a rat dural arteriovenous fistula model. *Exp Ther Med* **14**:5114–5120.
11. **Esposito F, Grimod G, Cavallo LM, Lanterna L, Birolfi F, Cappabianca P.** 2013. Collagen-only biomatrix as dural substitute: What happened after a 5-year observational follow-up study. *Clin Neurol Neurosurg* **115**:1735–1737. <https://doi.org/10.1016/j.clineuro.2013.03.013>.
12. **Fink BR, Walker S.** 1989. Orientation of fibers in human dorsal lumbar dura mater in relation to lumbar puncture. *Anesth Analg* **69**:768–772. <https://doi.org/10.1213/0000539-198912000-00014>.
13. **Greenberg RW, Lane EL, Cinnamon J, Farmer P, Hyman RA.** 1994. The cranial meninges: anatomic considerations. *Semin Ultrasound CT MR* **15**:454–465. [https://doi.org/10.1016/S0887-2171\(05\)80017-4](https://doi.org/10.1016/S0887-2171(05)80017-4).
14. **Haines DE, Harkey HL, al-Mefty O.** 1993. The “subdural” space: a new look at an outdated concept. *Neurosurgery* **32**:111–120. <https://doi.org/10.1227/00006123-199301000-00017>.
15. **Ito K, Horiuchi T, Oyanagi K, Nomiya T, Hongo K.** 2013. Comparative study of fibrin and chemical synthetic sealant on dural regeneration and brain damage. *J Neurosurg Spine* **19**:736–743. <https://doi.org/10.3171/2013.8.SPINE12998>.
16. **Jimenez Hamann MC, Sacks MS, Malinin TI.** 1998. Quantification of the collagen fibre architecture of human cranial dura mater. *J Anat* **192**:99–106. <https://doi.org/10.1046/j.1469-7580.1998.19210099.x>.
17. **Kawai H, Nakagawa I, Nishimura F, Motoyama Y, Park YS, Nakamura M, Nakase H, Suzuki S, Ikada Y.** 2014. Effectiveness of a new gelatin sealant system for dural closure. *Neurol Res* **36**:866–872. <https://doi.org/10.1179/1743132814Y.0000000342>.
18. **Kawai H, Nakagawa I, Nishimura F, Motoyama Y, Park YS, Nakamura M, Nakase H, Suzuki S, Ikada Y.** 2014. Usefulness

- of a new gelatin glue sealant system for dural closure in a rat durotomy model. *Neurol Med Chir (Tokyo)* **54**:640–646. <https://doi.org/10.2176/nmc.oa.2014-0005>.
19. **Knopp U, Christmann F, Reusche E, Sepehrnia A.** 2005. A new collagen biomatrix of equine origin versus a cadaveric dura graft for the repair of dural defects—a comparative animal experimental study. *Acta Neurochir (Wien)* **147**:877–887. <https://doi.org/10.1007/s00701-005-0552-0>.
  20. **Krasnov VV, Stogov MV, Silant'eva TA, Kubrak NV, Kireeva EA.** 2018. A technique for in vitro studying of the permeability of the spinal cord dura mater. *Bull Exp Biol Med* **164**:402–403. <https://doi.org/10.1007/s10517-018-3999-8>.
  21. **Lewis KM, Sweet J, Wilson ST, Rousselle S, Gulle H, Baumgartner B.** 2018. Safety and efficacy of a novel, self-adhering dural substitute in a canine supratentorial durotomy model. *Neurosurgery* **82**:397–406.
  22. **Mack J, Squier W, Eastman JT.** 2009. Anatomy and development of the meninges: implications for subdural collections and CSF circulation. *Pediatr Radiol* **39**:200–210. <https://doi.org/10.1007/s00247-008-1084-6>.
  23. **MacManus DB, Pierrat B, Murphy JG, Gilchrist MD.** 2017. Protection of cortex by overlying meninges tissue during dynamic indentation of the adolescent brain. *Acta Biomater* **57**:384–394. <https://doi.org/10.1016/j.actbio.2017.05.022>. PubMed
  24. **Nabeshima S, Reese TS, Landis DM, Brightman MW.** 1975. Junctions in the meninges and marginal glia. *J Comp Neurol* **164**:127–169. <https://doi.org/10.1002/cne.901640202>.
  25. **Nagel SJ, Reddy CG, Frizon LA, Chardon MK, Holland M, Machado AG, Gillies GT, Howard MA 3rd, Wilson S.** 2018. Spinal dura mater: biophysical characteristics relevant to medical device development. *J Med Eng Technol* **42**:128–139. <https://doi.org/10.1080/03091902.2018.1435745>.
  26. **Nishihira S, McCaffrey TV.** 1988. The use of fibrin glue for the repair of experimental CSF rhinorrhea. *Laryngoscope* **98**:625–627. <https://doi.org/10.1288/00005537-198806000-00009>.
  27. **Oxley TJ, Opie NL, Rind GS, Liyanage K, John SE, Ronayne S, McDonald AJ, Dornom A, Lovell TJH, Mitchell PJ, Bennett I, Bauquier S, Warne LN, Steward C, Grayden DB, Desmond P, Davis SM, O'Brien TJ, May CN.** 2018. An ovine model of cerebral catheter venography for implantation of an endovascular neural interface. *J Neurosurg* **128**:1020–1027. <https://doi.org/10.3171/2016.11.JNS161754>.
  28. **Ozsisik PA, Inci S, Soylemezoglu F, Orhan H, Ozgen T.** 2006. Comparative dural closure techniques: a safety study in rats. *Surg Neurol* **65**:42–47. <https://doi.org/10.1016/j.surneu.2005.04.047>.
  29. **Patel N, Kirmi O.** 2009. Anatomy and imaging of the normal meninges. *Semin Ultrasound CT MR* **30**:559–564. <https://doi.org/10.1053/j.sult.2009.08.006>.
  30. **Rhalmi S, Charette S, Assad M, Coillard C, Rivard CH.** 2007. The spinal cord dura mater reaction to nitinol and titanium alloy particles: a 1-year study in rabbits. *Eur Spine J* **16**:1063–1072. <https://doi.org/10.1007/s00586-007-0329-7>.
  31. **Sandoval- Sánchez JH, Ramos- Zúñiga R, de Anda SL, López-Dellamary F, Gonzalez- Castañeda R, Ramírez-Jaimes Jde L, Jorge-Espinoza G.** 2012. A new bilayer chitosan scaffolding as a dural substitute: experimental evaluation. *World Neurosurg* **77**:577–582. <https://doi.org/10.1016/j.wneu.2011.07.007>.
  32. **Schachenmayr W, Friede RL.** 1978. The origin of subdural neomembranes. I. Fine structure of the dura-arachnoid interface in man. *Am J Pathol* **92**:53–68.
  33. **Vandersteene J, Baert E, Schauvliege S, Vandeveldel K, Dewaele F, De Somer F, Van Roost D.** 2018. A non-hydrocephalic goat experimental model to evaluate a ventriculosinus shunt. *Lab Anim* **52**:504–514. <https://doi.org/10.1177/0023677217753976>.
  34. **Yu JC, McClintock JS, Gannon F, Gao XX, Mobasser J-P, Sharawy M.** 1997. Regional differences of dura osteoinduction: squamous dura induces osteogenesis, sutural dura induces chondrogenesis and osteogenesis. *Plast Reconstr Surg* **100**:23–31. <https://doi.org/10.1097/00006534-199707000-00005>.